Spectroscopic Study on Morphology Evolution in Polymer Blends

Tomoko Hashida, Young Gyu Jeong, Ying Hua, and Shaw Ling Hsu*

Polymer Science and Engineering Department and Materials Research Science and Engineering Center, University of Massachusetts (Amherst), Amherst, Massachusetts 01003

Charles W. Paul

National Starch, Bridgewater, New Jersey 08807

Received December 6, 2004; Revised Manuscript Received January 31, 2005

ABSTRACT: The morphological development of crystallizable polymer blends has been investigated using optical microscopy and infrared and Raman spectroscopy. Both binary and ternary blends were studied. In each case, a crystallizable polyester, either poly(hexamethylene adipate) (PHMA) or poly(hexamethylene sebacate) (PHMS), is mixed with noncrystallizable polyether, poly(propylene glycol) (PPG). Although they possess similar chemical structures, PHMA and PHMS exhibit very different miscibility behavior. In ternary blends, an acrylate, poly(methyl methacrylate and *n*-butyl methacrylate) [P(MMAnBMA)], is also incorporated in the mixture. With the high spatial resolution achievable (∼1 μm^2), the composition distribution can be carried out using a micro-Raman instrument. Specific Raman features associated with polyesters have been established. For immiscible PPG/PHMA blends, the composition and distribution within PHMA-rich and PHMA-poor phases are characterized. The exact composition in each phase has been obtained by analyzing Raman data obtained. Additionally, on the basis of the measured intensity for conformation-sensitive Raman peaks, the distribution of crystallites within each phase has been characterized. The third relative immobile acrylate component is extremely effective in changing the overall blend morphology.

Introduction

Polymer blends involving a crystallizable component are utilized in a large array of applications.[1] The morphological development in these systems is complex since both phase separation and crystallization may occur concurrently. In fact, the crystallization process is directly related to the composition variation associated with the phase separation process. Because of the difficulty in treating the two interrelated processes, the data in the literature are generally divided into two groups. One deals with the phase separation process and the other with characterization of crystalline units. Few studies relate the crystallization process to the miscibility behavior of the blends.

Practically speaking, crystalline features, such as degree of crystallinity, crystallite size, or crystalline perfection, are important considerations in determining the physical properties of polymer blends.[2,3] In our laboratory, we focus on polyurethane-based reactive adhesives consisting of noncrystallizable polyether and crystallizable polyester reactive blends.[4] Curing kinetics is therefore highly dependent on the ability of water molecules to diffuse into and through various morphological features and is greatly affected by the degree of crystallinity in such reactive blends.[5] In previous studies we established that the phase behavior of various crystallizable polyesters can vary dramatically with small differences in polymer structure. For example, blends involving poly(hexamethylene adipate) (PHMA) form a miscible phase at much higher temperature in comparison to poly(hexamethylene sebacate) (PHMS). These polyesters, although similar in chemical structure, exhibit different miscibility behavior when blended with a noncrystallizable polyether such as poly(propylene glycol) (PPG).[4] Consequently, the morphology formed is significantly different.[4] The PHMA system generally forms large domains. In contrast, as shown below, PHMS systems usually form small dispersed domains. Crystalline features, such as degree of crystallinity or crystal thickness, in each case are different as well.

Despite the great expectation of morphology control by miscibility, few fundamental studies exist on the crystallization in polymer blends in relation to miscibility. This may be due to the difficulty in obtaining the rigorous crystal growth rate. Optical microscopy and thermal measurements have often been used for studies on isothermal crystallization in blends.[6−8] It is difficult to obtain quantitative crystallization rates using optical microscopy because crystalline droplets must be sufficiently large for observation and crystallization typically occurs very quickly. In thermal measurements, the degree of crystallinity is obtained as a function of crystallization time. Rapid quench is required, and recrystallization via a heating process is unavoidable. X-ray diffraction measurements detect the exact crystalline structure. However, the diffraction intensity is insufficient for evaluation of blend crystallization kinetics in a short time interval.

To obtain rigorous crystallization kinetics and morphological features, we employed vibrational spectroscopy, both infrared and Raman, to characterize the crystallization process in various binary and ternary blends of interest. Fourier transform infrared spectroscopy can detect the conformational order of crystallizable polymer with high temporal resolution (∼seconds). We assume that the conformational ordering process is representative of crystallization development. Because of rapid improvements in Raman microscopes with an incident excitation beam size on the order of 1 μm^2, it

* To whom correspondence should be addressed; Tel: 413-577-1125; Fax: 413-545-0082; E-mail: slhsu@polysci.umass.edu.

10.1021/ma047492a CCC: $30.25
Published on Web 03/05/2005

is also possible to achieve high spatial resolution. Vibrational spectroscopy can then be employed to measure composition variation in phase-separated structures of various polymer blends.[9] Rather than an overall optical micrograph, a "map" of individual polymer components distributed in the various phases is obtained. On the basis of conformationally sensitive bands, it is also possible to measure crystallite formation and distribution within each morphological structure.

The presence of configurational defects, end groups, solvent molecules, and other polymer component all affect polymer crystallization behavior.[10−12] Analysis of crystallization in blends must consider the ability to nucleate and segmental mobility.[13] Crystallization kinetics must obviously then depend on the localized concentration of the crystallizable component.[13,14] It is also plausible that polymer crystals may nucleate at the phase boundary. One most difficult aspect in treating crystallization kinetics in polymer blends is the lack of knowledge regarding segmental dynamics within blends.[15] Segmental mobility is crucial for understanding transport behavior of chains participating in the crystallization process. There is no doubt, however, that the crystallization behavior directly relates to miscibility behavior.

To control viscosity of the reactive blends at elevated temperatures, a random acrylic copolymer of poly(methyl methacrylate and *n*-butyl methacrylate) [P(MMAnBMA)] is typically included. The glass transition temperature (T_g) of this copolymer is relatively high at 85.3 °C. Previous studies have shown this component to be quite important in determining overall blend physical properties.[4] Its role in morphology formation is, however, unclear. Undoubtedly, because of its high glass transition temperature, the mobility of other chains may be significantly perturbed. It is then expected that the crystallization behavior of the polyester component is further modified.

The principal objective of this study is to utilize the micro-Raman technique to map the chemical composition of each phase in both binary and ternary blends. It is possible to directly obtain the composition difference in miscible vs immiscible blends. We shall also address how spectroscopy contributes to measurement of crystallization kinetics and relate the mechanism to miscibility behavior.

Experimental Section

Poly(propylene glycol) (PPG) [M_n = 1887 g/mol], poly(hexamethylene adipate) (PHMA) [M_n = 1575 g/mol], and poly(hexamethylene sebacate) (PHMS) [M_n = 1371 g/mol] were used for polyether/polyester binary blends. Equilibrium melting points ($T_m°$) are 58 °C for PHMA and 70 °C for PHMS.[16,17] Both polymers are terminated with primary OH groups. The chemical structures of PHMA and PHMS are shown in Scheme 1.

In the ternary blend system, a random acrylic copolymer of poly(methyl methacrylate and *n*-butyl methacrylate) [P(MMAnBMA); M_n = 18 841 g/mol] was mixed with polyester and polyether. The glass transition temperature (T_g) of P(MMAnBMA) is 85.3 °C.

The isothermal crystallization and melting behavior of polyester were studied as follows. The polyesters were heated at 100 °C for 1 min and rapidly cooled to the crystallization temperature. For all comparison analyses, the degree of supercooling is used in order to take into account the difference in melting temperature between the two polyesters.

The morphology development of blends was observed at room temperature using an Olympus Vanox optical microscope equipped with a Kodak EASYSHARE LS443 zoom digital camera. Thermal measurements were carried out using a TA Instruments DSC Q 100 instrument. The heating rate was maintained at 10 °C/min. The degree of polyester crystallinity was estimated by comparing the melting enthalpy (ΔH) of an isothermally crystallized sample with the equilibrium melting enthalpy of polyester (ΔH^0), as shown in Table 1.[16,17]

Scheme 1. Chemical Structures of Polyesters Used in This Study

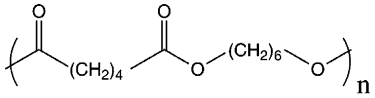

Poly(hexamethylene adipate) [PHMA]

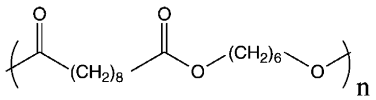

Poly(hexamethylene sebacate) [PHMS]

Table 1. Thermal Data of Polyester and the Degree of Crystallinity at ΔT = 13 °C

	T_m^0/°C	ΔH^0/J g^{-1}	ΔH/J g^{-1} (ΔT = 13 °C)	crystallinity/% (ΔT = 13 °C)
PHMA	58[a]	151[a]	66.6	44
PHMS	70[a,b]	134[a,b]	48.4	36

[a] Reference 16. [b] Reference 17.

Time-resolved infrared spectral measurements were obtained using a Perkin-Elmer 2000 FT-IR spectrometer. The spectral resolution was maintained at 4 cm^{-1}. Infrared spectra were obtained every 14 s in order to follow the crystallization process at specific temperatures. In each case, the molten film is rapidly quenched to the crystallization temperatures in a specially designed cell.

The compositional distribution of blends was characterized using a laser confocal Raman spectrometer (Jobin Yvon HORIBA LabRam HR800 Raman microscope) with CCD detector. The spectral resolution was kept at 1 cm^{-1}. This instrument is equipped with a conical focus capable of high spatial resolution, ~1 μm^2. The morphology at an identical spot can be obtained using both the optical microscope and Raman instrument.

The intensities of infrared bands and Raman peaks characteristic of the components were primarily obtained by integrating the area of bands. When the bands for analyses overlapped other bands, the curve fitting was performed using the MIDAC GRAMS/32 program. It uses a combination of Lorentzian and Gaussian to fit the peak above the baseline connecting two minima until iterations stop. The subtraction technique was used to obtain the local composition using Raman data. As shown below, the Raman spectra of pure components were subtracted from spectra obtained in different phases. The coefficient to subtract the component was considered as its local composition.

Results and Discussion

Homopolymer. The degree of polyester crystallinity was estimated by comparing the melting enthalpy (ΔH) of an isothermally crystallized sample with the equilibrium melting enthalpy of polyester (ΔH^0), as shown in Table 1.[16,17] The degree of crystallinity at ΔT of 13 °C is 44% for PHMA and 36% for PHMS. Since the structures of the two polyesters are so similar, the expectation is that their crystallization behavior would be similar as well. Their equilibrium melting temperature differs somewhat. This difference has been taken into account in the crystallization analysis by using an identical degree of supercooling, ΔT, defined by $T_m° - T_c$.

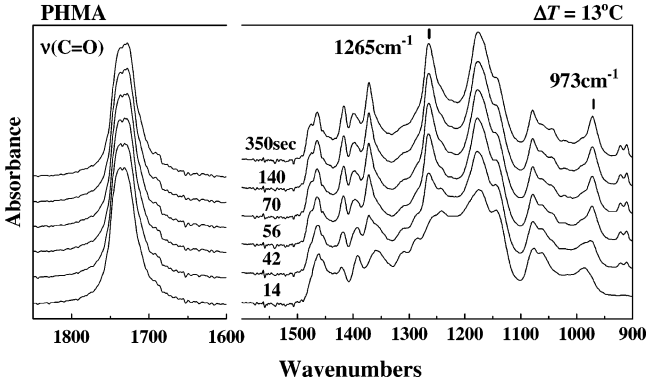

Figure 1. Time dependence of infrared spectra for PHMA at the degree of supercooling (ΔT) of 13 °C.

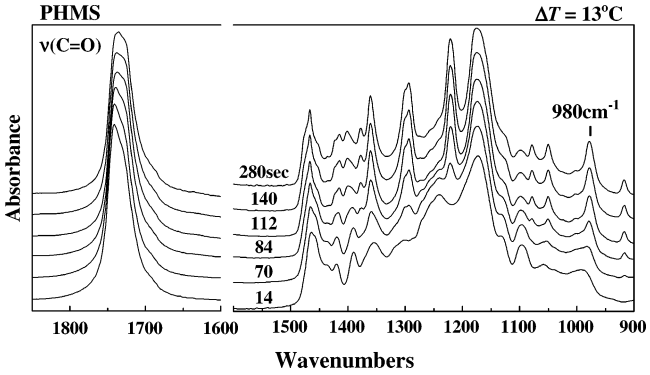

Figure 2. Time dependence of infrared spectra for PHMS at the degree of supercooling (ΔT) of 13 °C.

The infrared spectra obtained for PHMA as a function of time are shown in Figure 1. These data are obtained for a degree of supercooling of 13 °C. The infrared-active bands at 973 and 1265 cm^{-1} increase in intensity as a function of time. These bands, assignable to CH_2 skeletal deformation vibrations, are sensitive to the conformational order.[18] In contrast, the C=O polyester stretching bands at 1733 cm^{-1} do not change during crystallization. Similarly, PHMS infrared data obtained at the same experimental conditions are shown in Figure 2. In this case, the CH_2 deformation band shifts to 980 cm^{-1}. The integrated intensities of 973 cm^{-1} PHMA bands and 980 cm^{-1} PHMS bands, normalized by the intensity of C=O stretching bands at 14 s, are plotted with time in Figure 3. Initially, up to 14 s, and, as expected, there is no evidence of crystallinity. The increase in the degree of crystallinity follows a similar trend for both polyesters before reaching a plateau value fairly quickly. Since the degrees of crystallinity are known for the two homopolymers, it is then possible to correlate the infrared intensity to the degree of crystallinity.

Composition Distribution. The morphology development of PPG/PHMA (5/1) immiscible blends during cooling from the molten state to room temperature is shown in Figure 4. A phase-separated structure clearly exists, even in the melt. Crystallization starts at the interface between a rich and poor phase and then grows inward. The spherelike rich phase crystallizes first and is then followed by the poor phase. Crystallization proceeds in the latter region until the rich phase has completely crystallized. The crystallization rates of the two phases differ dramatically. The crystallization process for the PPG/PHMS (5/1) blend is shown in Figure 5. This miscible blend exhibits a very different

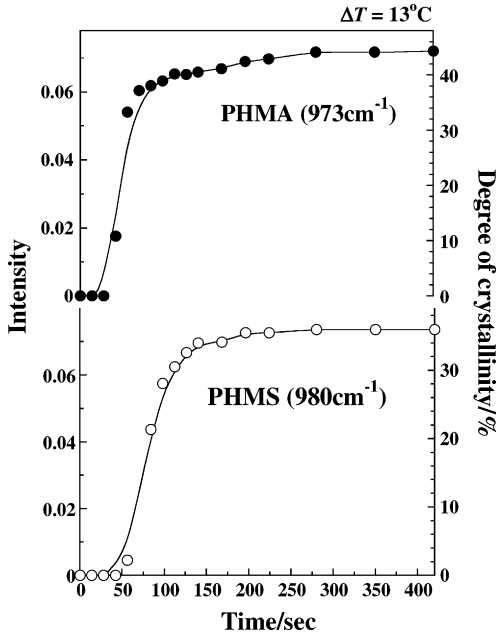

Figure 3. Crystallization kinetics and the degree of crystallinity of PHMA and PHMS at the degree of supercooling (ΔT) of 13 °C. The normalized intensities of 973 cm^{-1} PHMA and 980 cm^{-1} PHMS crystalline bands are correlated with the degree of crystallinity obtained by thermal analysis.

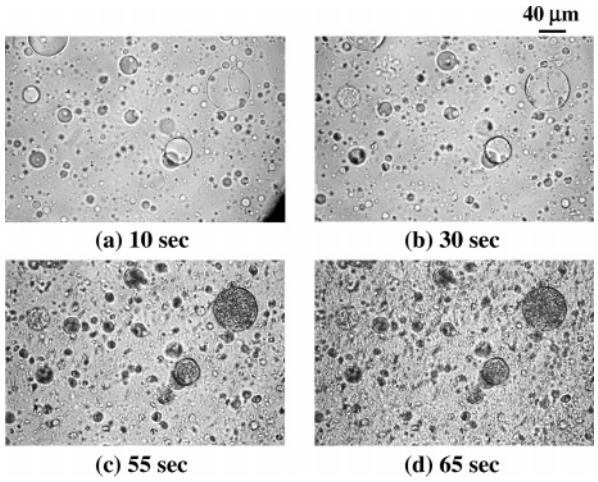

Figure 4. Optical micrographs for PPG/PHMA (5/1) blends cooled from melt to the room temperature. The morphology development of PPG/PHMA (5/1) blends at (a) 10, (b) 30, (c) 55, and (d) 65 s.

crystallization process in comparison to an immiscible blend. The final morphology obtained is fairly homogeneous, consisting of small domains. The overall crystallization process for miscible blends is clearly much slower than the rich phase in immiscible blends. These observations demonstrate that the environment in which the crystallizable component exists can significantly influence crystallization kinetics.

To probe the composition of each phase in the phase-separated morphology of PPG/PHMA immiscible blends, confocal Raman spectroscopy capable of high spatial resolution was employed. The beam size of the excitation laser focused on the sample is approximately 1 μm^2, sufficiently small to reveal local composition of the rich phase generally 40−80 μm in diameter. Spectra obtained at various regions of the immiscible PHMA blends are shown in Figure 6. One is obtained in the center of the rich phase, one at the interface, and one

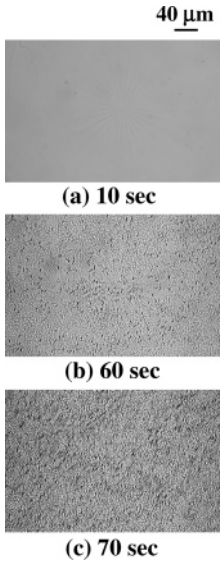

Figure 5. Optical micrographs for PPG/PHMS (5/1) blends cooled from melt to the room temperature. The morphology development of PPG/PHMS (5/1) blends at (a) 10, (b) 60, and (c) 70 s.

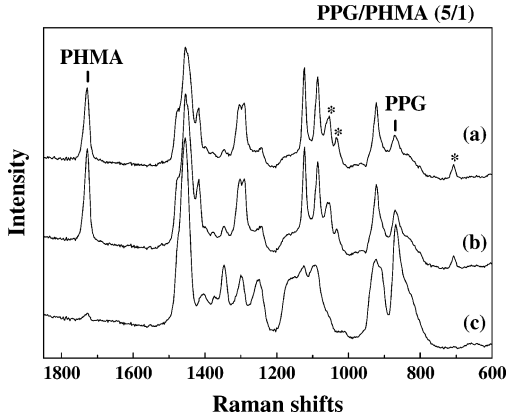

Figure 6. Raman spectra taken (a) at the center of PHMA-rich phase, (b) near interface inside PHMA-rich phase, and (c) in PHMA-poor phase for PPG/PHMA (5/1) immiscible blends.

in the poor phase. The intensity of the C=O stretching vibration associated with PHMA at 1729 cm^{-1} is much stronger in the PHMA-rich phase while the PHMA-poor phase shows a strong band at 868 cm^{-1} assignable to PPG. Based on the integral intensity of this band, the relative concentration of PHMA in the rich phase is almost 12 times the poor phase. To estimate the PHMA concentration in each phase, the PPG Raman spectrum was subtracted from both those obtained for the rich and poor regions. The results are consistent with each other and with PHMA. These are shown in Figure 7. The coefficient used to eliminate the PPG contribution for the rich phase is 0.28. This implies there is a 72 ± 2% PHMA concentration in PHMA-rich phases. In contrast, the PHMA concentration in PHMA-poor phases is 6−7%. These local PHMA concentrations obtained using the subtraction technique are consistent with the intensity ratio of the C=O stretching vibration found at 1729 cm^{-1}.

The Raman spectra were obtained at two different phases for the PPG/PHMA (1/1) blend. Using a similar subtraction technique, the rich phase was found to consist of 72−78% PHMA. In contrast, the poor phase has 17−20% PHMA. These results are also consistent

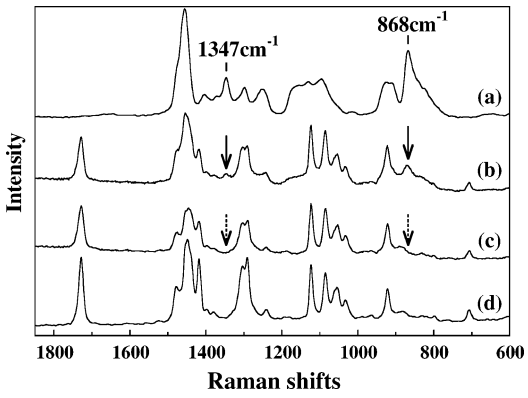

Figure 7. Raman spectra of (a) PPG, (b) PHMA-rich phase in PPG/PHMA (5/1) blends, (c) the subtracted result of PHMA-rich phase spectra minus PPG spectra, and (d) PHMA.

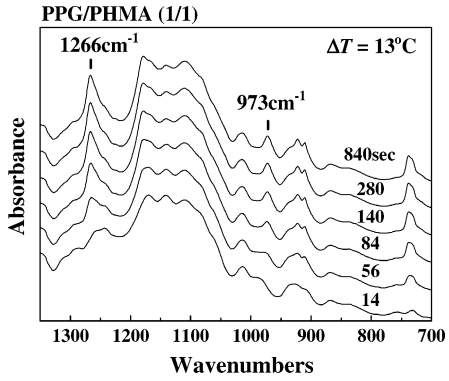

Figure 8. Time dependence of infrared spectra for PPG/PHMA (1/1) blends at the degree of supercooling (ΔT) of 13 °C.

with the intensity ratio measured for the integrated intensity of the C=O stretching vibration. It is clear that for PPG/PHMA immiscible blends there are regions with high concentration of PHMA although the overall blend composition can vary significantly. For PPG/PHMS miscible blends, polyester is homogeneously distributed in the sample. The distribution of the crystallizable polyester is very different between immiscible and miscible blends.

Crystallization Kinetics. The time dependence of infrared spectra obtained for PPG/PHMA (1/1) immiscible blends at ΔT = 13 °C is shown in Figure 8. Crystalline features are totally absent within the initial 14 s. The intensity of the 973 and 1266 cm^{-1} bands then increases with time. The time-dependent spectra of PPG/PHMS (1/1) at ΔT of 13 °C were also obtained. The intensity of the PHMS crystalline band at 980 cm^{-1} increased in the cooling process. The 973 cm^{-1} PHMA band and the 980 cm^{-1} PHMS band used for analysis are sensitive to conformational order. Unlike most infrared-active features, they do not overlap with polyether bands.

Similar to the analysis carried out for homopolymers, the integrated intensity of polyester crystalline bands is normalized to C=O stretching bands and can be used to follow crystallization of polyesters in various blends (Figure 9). The degree of crystallinity was calculated as shown above by correlating the intensity of infrared bands to the degree of crystallinity measured using thermal measurements as demonstrated in Figure 3. The degree of crystallinity obtained using spectroscopic data probably has uncertainties such as ±1%.

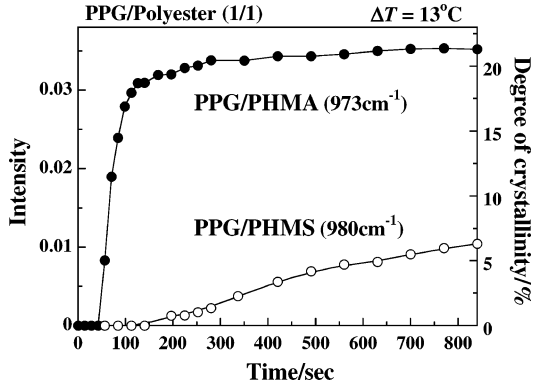

Figure 9. Comparison of crystallization kinetics between PPG/PHMA (1/1) immiscible blends and PPG/PHMS (1/1) miscible blends at the degree of supercooling (ΔT) of 13 °C; time dependence of normalized intensities of 973 cm^{-1} PHMA and 980 cm^{-1} PHMS crystalline bands correlated with the degree of crystallinity obtained by thermal analysis.

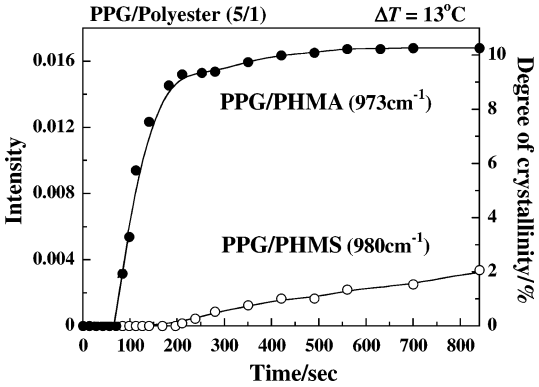

Figure 10. Comparison of crystallization kinetics between PPG/PHMA (5/1) immiscible blends and PPG/PHMS (5/1) miscible blends at the degree of supercooling (ΔT) of 13 °C; time dependence of normalized intensities of 973 cm^{-1} PHMA and 980 cm^{-1} PHMS crystalline bands correlated with the degree of crystallinity obtained by thermal analysis.

It is obvious that crystallization kinetics and the ultimate degree of crystallinity depend on miscibility behavior. The PPG/PHMS miscible blends show much slower crystallization kinetics although the overall blend composition is identical. The measured degrees of crystallinity are approximately 22 and 6% for PPG/PHMA (1/1) and PPG/PHMS (1/1) blends, respectively. As shown in Figure 3, the crystallization kinetics measured for the two homopolymers is nearly identical at the same degree of supercooling. In the blend with PPG, however, the crystallization kinetics are totally different. Miscible blends exhibit slower crystallization kinetics and lower degrees of crystallinity.

The crystallization kinetics of the two blends with different overall composition is shown in Figure 10. In this case, the relative ratio of PPG to polyester is five to one. The integrated intensity of the conformational sensitive bands and calculated degree of crystallinity also exhibit tremendous differences in crystallization kinetics and degree of crystallinity achieved. The degree of crystallinity obtained is approximately 10 and 2% for PPG/PHMA and PPG/PHMS, respectively. Although the PPG/PHMA (5/1) immiscible blends crystallize to the degree of crystallinity of 9−10% in 200 s, the degree of crystallinity of PPG/PHMS (5/1) miscible blends is almost a negligible amount of 2% at 840 s.

Various Raman-active peaks can be used to characterize the degree of crystallinity of different regions in the blend samples. For example, we found the PHMA peaks at 707, 1033, and 1055 cm^{-1} (marked with asterisks in Figure 6) to be sensitive to conformational order, expressing the degree of crystallinity. Similarly, these bands in conjunction with thermal measurements can reveal the degree of crystallinity in the localized regions of various blends. Generally speaking, the degree of crystallinity is much higher in the polyester-rich domains vs the polyester-poor regions. The differences can be measured using Raman spectroscopy. The PHMA-poor phase in PPG/PHMA (5/1) blends did not exhibit any crystallinity (Figure 6). Therefore, the crystallization kinetics obtained for PPG/PHMA (5/1) blends in Figure 10 represents the crystallization process of PHMA-rich phases. Unlike PPG/PHMA (5/1) blends, there is some crystallinity in the PHMA-poor phase of PPG/PHMA (1/1) blends.

The PHMA-rich phase in PPG/PHMA (5/1) blends is found to contain over 70% PHMA. In contrast, PHMS is homogeneously distributed in the corresponding blend. Thus, the crystallization behavior of PPG/polyester (5/1) blends in Figure 10 reflects effects of different composition distribution on the crystallization process. The distribution of crystallizable components is very different between immiscible and miscible blends. The crystallization behavior in each type of polymer blends also differs considerably.

Miscible vs Immiscible Blends. As demonstrated above, crystallization behavior such as crystallization kinetics and the degree of crystallinity was found to be very different between immiscible and miscible blends. PPG/PHMS miscible blends exhibit slower crystallization kinetics and lower degrees of crystallinity in comparison to the crystallizable component in immiscible blends. The distribution of crystallizable components will influence both nucleation and transport behavior of crystallizable units. We are unaware of any theory to explain these differences on a quantitative basis. On the other hand, many theories dealing with nucleation and chain dynamics can be used to qualitatively describe the observed differences. Both aspects affect the two crucial aspects of usual crystallization processes as defined previously.[19,20]

The nucleation rate should be faster with higher concentration of crystallizable units at the crystal growth front. Various aspects of this process have been previously considered.[12] The transport dynamics of crystallizable units to the crystallite−liquid interface can be considered using the reptation model.[19,21] This expression is adequate to describe the rate that polymers are to be drawn from the random-coil melt onto the growth front. The effective transport rate, v_r, is

$$v_r = \frac{f_c}{\zeta_r} \tag{1}$$

where f_c is the force for pushing molecules to the growth front and ζ_r is the friction coefficient associated with the reptation, corresponding to the segmental size in the reptation model. The transport behavior in the crystal growth process is equivalent to the reptation velocity of eq 1.

The correlation length ξ_r, defining the average distance between neighboring contact points of crystallizable polymer chains, can be considered as a diffusion unit in the reptation model.[22] This diffusion unit will be smaller at higher concentration of crystallizable

Scheme 2. Schematic Illustration of Entangled Polymer Chains in the Molten Sate of Blends[a]

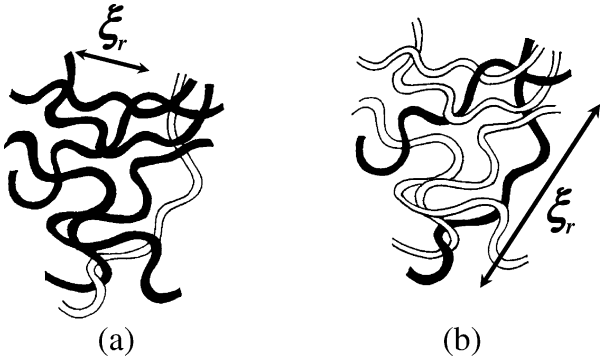

[a] The average distance between contacting points of crystallizable polymer chains (black) is ξ_r. (a) expresses the high composition of crystallizable component, and (b) does the low composition of that.

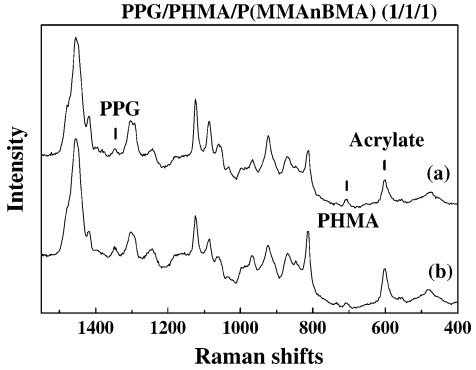

Figure 11. Raman spectra taken (a) at the center of PHMA-rich phase and (b) in PHMA-poor phase for PPG/PHMA/P(MMAnBMA) (1/1/1) blends cooled from 120 °C.

component, as illustrated in Scheme 2. The frictional coefficient ζ_r increases with ξ_r. Therefore, the transport behavior of crystallizable components in blends will increase with the concentration of crystallizable components.

Effects of the Presence of an Immobile Component. The presence of the immobile acrylic copolymer, poly(methyl methacrylate and *n*-butyl methacrylate) [P(MMAnBMA)], with high glass transition temperature (T_g) at 85.3 °C, is known to influence the phase behavior of PPG/PHMA.[4] The obtained phase diagram indicates the PPG/PHMA/P(MMAnBMA) (1/1/1) ternary blend is miscible at 140 °C and generates phase separation with decreasing temperature.[4] Using our Raman technique, the composition distribution of the phase-separated structure obtained for ternary blends is shown in Figure 11. Raman spectra were taken at the center of the PHMA-rich phase (a) and in the PHMA-poor phase (b) of PPG/PHMA/P(MMAnBMA) (1/1/1) blends. Raman peaks at 601, 707, and 1347 cm^{-1} are analyzed for P(MMAnBMA), PHMA, and PPG, respectively. Only these Raman peaks do not overlap with other components. The intensity ratio of the PHMA peak at 707 cm^{-1} of the PHMA-rich phase to the PHMA-poor phase is 1 to 0.7, showing a more evenly distributed polyester in ternary blends as compared to the binary system. The composition of acrylic copolymer is 40% higher in the PHMA-poor phase. Compared with PPG/PHMA binary blends, all ternary blends with this relatively immobile component exhibit a more homogeneously distributed structure.

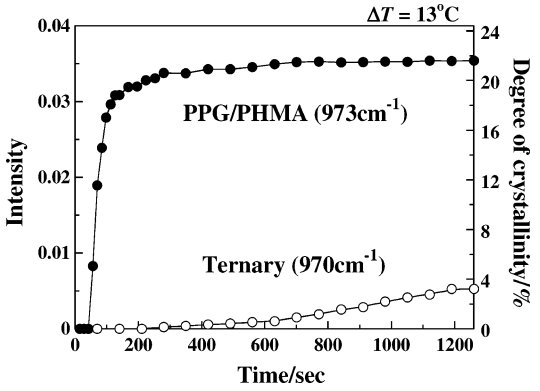

Figure 12. Comparison of crystallization kinetics between PPG/PHMA (1/1) binary blends and PPG/PHMA/P(MMAnBMA) (1/1/1) ternary blends at the degree of supercooling (ΔT) of 13 °C; time dependence of normalized intensities of PHMA crystalline bands at 973 and 970 cm^{-1} correlated with the degree of crystallinity obtained by thermal analysis.

The infrared spectra were obtained as a function of time for the PPG/PHMA/P(MMAnBMA) (1/1/1) ternary blends kept at 13 °C of supercooling (ΔT). As the sample cools from 120 °C, the intensity of PHMA crystalline bands at 970 cm^{-1} increases in intensity and can be used for analysis. Comparison of PHMA crystallization kinetics between PPG/PHMA (1/1) binary blends and PPG/PHMA/P(MMAnBMA) (1/1/1) ternary blends at the same degree of supercooling (ΔT = 13 °C) is shown in Figure 12. The degree of crystallinity was estimated by measuring the infrared band intensity of PHMA, as shown in Figure 3. The contribution of the acrylic component to the polyester C=O stretching component (1734 cm^{-1}) is eliminated by use of the subtraction technique. Based on data obtained for the homopolymer, the relative intensity of the C=O stretching (1730 cm^{-1}) to the 750 cm^{-1} band is 7.9. Since the acrylic copolymer band at 750 cm^{-1} overlaps less with other components, the integrated intensity was obtained by curve fitting. The crystal growth rate of PHMA in the ternary blends is extremely slow as compared with PPG/PHMA binary blends. While the degree of crystallinity for PPG/PHMA binary blends reaches 20% at 200 s, ternary blends continue to crystallize even at 1200 s. The degree of crystallinity at that point is only 3−4%. The reduced chain mobility slows the crystal growth process since the composition distribution of ternary blends is more homogeneous even in the phase-separated structure. The high glass transition temperature (T_g) of acrylic copolymer affects both phase separation and the crystallization process. It is clear that incorporation of the relative immobile component affects both composition distribution and morphology distribution.

Conclusions

The composition distribution in various binary and ternary blends has been characterized by infrared and Raman spectroscopy in conjunction with optical microscopic and thermal studies. Different composition distributions due to miscibility were found to change the crystallization process and subsequent morphological features in crystallizable/noncrystallizable polymer blends. The blends studied involve polyesters of PHMA and PHMS and noncrystallizable components of PPG. Although these two polyesters have similar chemical structures, PPG/PHMA blends are immiscible while PPG/PHMS blends are miscible. The observed morpho-

logical features are quite different. PPG/PHMA blends exist as a phase-separated morphology. In contrast, PPG/PHMS blends have a homogeneous structure.

On the basis of spectroscopic features consistent with crystalline structure, the overall crystallization process in both systems has been characterized. These data confirm the significant difference in the crystallization rate observed in optical microscopy. The phase-separated PPG/PHMA structures crystallize faster than miscible PPG/PHMS systems. In PPG/PHMA immiscible blends the crystallization rate in the PHMA-rich phase is faster than the PHMA-poor phase. Detailed morphology was characterized using high-resolution laser confocal Raman spectroscopy. The composition of the rich and poor phases was established in a quantitative fashion. For example, in the rich phase of a five to one (PPG to PHMA) blend, polyester can be as high as 72 %. In contrast, the poor phase has only 6% polyester. It was also possible to map the degree of crystallinity at various locations.

Virtually all crystalline features, if present, grew quickly in the rich phase. When blends involve a relative immobile component such as the acrylic copolymer of P(MMAnBMA), the phase behavior of the phase diagram changed significantly. Previously immiscible PPG/PHMA/P(MMAnBMA) blends became miscible. The composition distribution in ternary blends obtained using laser confocal Raman spectroscopy is more homogeneous even in the phase-separated structure. Optical micrograph and infrared spectral measurements exhibited smaller domains in the phase-separated morphology and much slower crystallization kinetics and lower degrees of crystallinity in ternary blends in comparison to PPG/PHMA (1/1) binary blends. Reduced chain mobility of components due to the high T_g component decreases the speed of phase separation and the crystallization process. Very different morphological features are therefore obtained. The morphology evolution in polymer blends requires fairly detailed analysis. No theory is currently available capable of such an explanation.

Acknowledgment. The authors thank the National Science Foundation-Environmental Protection Agency (TSE Grant #RD831636010) for financial support. We also appreciate a grant from National Starch, a subsidiary of ICI, for supporting this research.

References and Notes

(1) Plochocki, A. P. *Polymer Blends*; Academic Press: New York, 1978; Vol. 2.
(2) Schonhorn, H.; Ryan, F. W. *J. Polym. Sci., Part A-2: Polym. Phys.* **1968**, *6*, 231.
(3) Schonhorn, H. *J. Polym. Sci., Part B: Polym. Lett.* **1967**, *5*, 919.
(4) Duffy, D. J.; Stidham, H. D.; Hsu, S. L.; Sasaki, S.; Takahara, A.; Kajiyama, T. *J. Mater. Sci.* **2002**, *37*, 4851.
(5) Comyn, J.; Brady, F.; Dust, R. A.; Graham, M.; Haward, A. *Int. J. Adhes. Adhes.* **1998**, *18*, 51.
(6) Ong, C. J.; Price, F. P. *J. Polym. Sci., Part C: Polym. Symp.* **1977**, 59.
(7) Penning, J. P.; Manley, R. S. J. *Macromolecules* **1996**, *29*, 84.
(8) Qiu, Z. B.; Ikehara, T.; Nishi, T. *Polymer* **2003**, *44*, 3101.
(9) Kim, J. S.; Ho, P. K. H.; Murphy, C. E.; Friend, R. H. *Macromolecules* **2004**, *37*, 2861.
(10) Flory, P. J. *Principles of Polymer Chemistry*; Cornell University Press: Ithaca, NY, 1953.
(11) Nishi, T.; Wang, T. T. *Macromolecules* **1975**, *8*, 909.
(12) Gornick, F.; Mandelkern, L. *J. Appl. Phys.* **1962**, *33*, 907.
(13) Di Lorenzo, M. L. *Prog. Polym. Sci.* **2003**, *28*, 663.
(14) Cham, P. M.; Lee, T. H.; Marand, H. *Macromolecules* **1994**, *27*, 4263.
(15) Pathak, J. A.; Kumar, S. K.; Colby, R. H. *Macromolecules* **2004**, *37*, 6994.
(16) Aylwin, P. A.; Boyd, R. H. *Polymer* **1984**, *25*, 323.
(17) Omalley, J. J.; Stauffer, W. J. *J. Polym. Sci., Part A: Polym. Chem.* **1974**, *12*, 865.
(18) Snyder, R. G. *J. Chem. Phys.* **1965**, *42*, 1744.
(19) Hoffman, J. D.; Guttman, C. M.; Dimarzio, E. A. *Discuss. Faraday Soc.* **1979**, *68*, 177.
(20) Gedde, U. W. *Polymer Physics*; Kluwer Academic Publishers: Dordrecht, 1995.
(21) de Gennes, P. G. *J. Chem. Phys.* **1971**, *55*, 572.
(22) de Gennes, P. G. *Macromolecules* **1976**, *9*, 587.

MA047492A